Laminarization of minimal plane Couette flow: Going beyond the basin of attraction of turbulence

Genta Kawahara[a)]
Department of Aeronautics and Astronautics, Kyoto University, Kyoto 606-8501, Japan

(Received 22 December 2004; accepted 17 February 2005; published online 4 April 2005)

Laminarization of minimal plane Couette turbulence is achieved numerically through short-time imposition of weak spanwise system rotation. A laminarization strategy presented in this Letter is inspired by investigation of the phase-space structure in the vicinity of a recently found unstable periodic orbit [G. Kawahara and S. Kida, "Periodic motion embedded in plane Couette turbulence: regeneration cycle and burst," J. Fluid Mech. **449**, 291 (2001)]. The periodic orbit, which a turbulent state occasionally approaches, and its local stable manifold are found to form the separatrix between the basin of attraction of turbulent and laminar flows. The introduction of the slight rotation during its approach to the periodic orbit enables the state to go beyond the basin of attraction of the turbulence toward the laminar flow. The global stabilization of the unstable periodic orbit by the method of controlling chaos is also performed to accomplish the laminarization without waiting until the natural approach. © *2005 American Institute of Physics*.
[DOI: 10.1063/1.1890428]

Control of turbulent flows has long been a subject of great importance in a wide variety of engineering applications. Turbulent skin friction is, for example, a significant factor in total drag on commercial aircrafts and cargo ships, and its reduction is one of crucial technology for energy savings. Modern control theories have been applied to a reduction in skin-friction drag in numerically simulated turbulent channel flows,[1] and it has recently been reported that subcritical turbulent channel flow can be laminarized by use of nonlinear[2] or linear[3] optimal control theories. The optimal control in these studies is a systematic and sophisticated approach to laminarization with a remarkable drag reduction; however, the theories developed therein might be somewhat intricate.

Appealingly simple control strategies, that is, controlling chaos, have been extensively developed in low-dimensional nonlinear dynamical systems ever since the 1990 pioneer work of Ott *et al.*[4] It is known that an infinite number of unstable periodic orbits are embedded in a chaotic attractor, and in controlling chaos one of the embedded periodic orbits, which is more desirable than chaos, is stabilized by a variety of techniques.[4,5] The key idea of controlling chaos is to take advantage of the sensitivity of chaotic dynamics to initial conditions or parameter values, which implies that desired states can be produced by a small change in those conditions or values. Recently chaos control has been gradually carried out in high-dimensional systems, such as two-dimensional turbulence.[6] It is, however, difficult to find a nonlinear goal solution to the three-dimensional Navier–Stokes equation, and this is a serious obstruction to application of chaos-control strategies to near-wall turbulence.

Several possible candidates for nonlinear goal states have been obtained numerically in the past few years in plane Couette flow,[7–9] plane Poiseuille flow,[8,10] and autonomous wall flow.[11] They are three-dimensional unstable equilibrium or periodic solutions, and some of them have been shown to represent a less dissipative quiescent state with low skin-friction drag,[12] which could be a desirable goal of controlling chaos. In this study we discuss the gentle periodic orbit with low skin-friction drag, which is one of two periodic orbits found in plane Couette flow,[9] as an example of possible candidates for a drag reduction. The behavior, in phase space, of a turbulent state around this periodic orbit is examined to obtain a laminarization strategy for low-Reynolds-number minimal plane Couette flow. The periodic orbit will play a crucial role as an intermediary goal.

We perform direct numerical simulations of the incompressible Navier–Stokes equation, by using a spectral method, for the same minimal Couette turbulence as investigated by Hamilton *et al.*[13] A plane Couette system is known to be linearly stable at any Reynolds number, and so a laminar state has a basin of attraction in phase space. Therefore the state tends to laminar flow or turbulent one depending on an initial condition. The developed turbulent states are obtained from the long-time simulations from appropriate initial conditions. The numerical code for the simulations is the one in Ref. 9, and was developed by Toh (see Ref. 10). The dealiased Fourier and Chebyshev-polynomial expansions are employed in the wall-parallel directions (streamwise x and spanwise z), and in the wall-normal direction (y), respectively. The streamwise volume flux and the spanwise mean pressure gradient are, respectively, set to be zero. Numerical computations are carried out on 8448 ($=16\times33\times16$ in x, y, and z) grid points at Reynolds number $\mathrm{Re}\equiv Uh/\nu=400$, where U is half the difference of the two wall velocities, h is half the wall separation, and ν is the kinematic viscosity of fluid. The Reynolds number based on h and the mean friction velocity u_τ of turbulent flows is $\mathrm{Re}_\tau=34.1$. The streamwise

a)Electronic mail: gkawahara@kuaero.kyoto-u.ac.jp

and spanwise computational periods are $L_x/h=1.755\pi$ ($L_x^+=188$) and $L_z/h=1.2\pi$ ($L_z^+=129$), respectively. Hereafter the superscript $+$ indicates flow variables normalized by u_τ and ν. The grid spacing in the x, y, and z directions is $\Delta x^+=12$, $\Delta y^+=0.16$–3.3, and $\Delta z^+=8.1$, which is comparable to that in most direct numerical simulations. In the minimal Couette turbulence the spatial symmetries[7]—(i) the reflection with respect to the plane of $z=0$ and a streamwise shift by a half period $L_x/2$; (ii) the 180° rotation around the line $x=y=0$ and a spanwise shift by a half period $L_z/2$—have been observed to appear approximately without being imposed on the flow.[9] We compute turbulent flows with and without imposing these symmetries. They are also imposed on the periodic solution to be computed below. The turbulent solutions with the symmetries will not have translational invariance in the wall-parallel directions, so that we can strictly measure the distance in phase space between the periodic and turbulent states on the Poincaré section.

We recompute the time-periodic solution with low skin-friction drag in Ref. 9 with much higher accuracy by introducing the Newton–Raphson method. Let us consider the N-dimensional phase space spanned by all the N independent variables which are the Chebyshev coefficients for the mean streamwise and spanwise velocities, and the Fourier–Chebyshev coefficients for the wall-normal velocity and vorticity ($N\approx 1.5\times 10^4$). If we impose the symmetries (i) and (ii) on the flow, its dynamics can be described in the n-dimensional subspace ($n\approx N/4$). In the subspace the Poincaré section is defined by $\mathrm{Im}(\tilde{\omega}_{y1,2,0})=0$, where $\mathrm{Im}(\tilde{\omega}_{y1,2,0})$ is the imaginary part of the Fourier–Chebyshev coefficient of the wall-normal vorticity for the $2\pi/L_x$ streamwise wavenumber, the second-order polynomial, and the zero spanwise wavenumber. We obtain the periodic solution as a fixed point of an $(n-1)$-dimensional Poincaré map $\boldsymbol{f}(\boldsymbol{r})$, where $\boldsymbol{r}$ is an $(n-1)$-dimensional state vector on the Poincaré section. The Poincaré map is computed by the direct numerical simulation described above, and its Jacobian matrix $D_{\boldsymbol{r}}\boldsymbol{f}(\boldsymbol{r})$ is evaluated by a finite-difference approximation. We use the gentle periodic solution in Ref. 9 as an initial guess for the Newton–Raphson iteration with accuracy $\|\boldsymbol{f}(\boldsymbol{r})-\boldsymbol{r}\|/\|\boldsymbol{r}\|<10^{-9}$, where $\|\cdot\|$ denotes the Euclidean norm. The periodic motion has been observed at least in the range of $\mathrm{Re}=240$–500 (or $L_x/h=1.755\pi$–1.88π) for $L_x/h=1.755\pi$, $L_z/h=1.2\pi$, (or $\mathrm{Re}=400$, $L_z/h=1.2\pi$). In the following the periodic solution is investigated only at the same parameter values as those for the above-mentioned minimal turbulence.[13]

As already reported in Ref. 9, the turbulent state wanders chaotically in phase space and approaches occasionally the gentle periodic orbit with low wall shear. A similar approach to a quiescent equilibrium state has first been observed in a plane Poiseuille system.[10] Let us consider the normalized distance, $d_p=\|\boldsymbol{x}-\boldsymbol{x}_f\|/\|\boldsymbol{x}_f\|$, in the full N-dimensional phase space between the intersection of the periodic orbit $\boldsymbol{x}_f$, and that of the orbit for the symmetric turbulent flow $\boldsymbol{x}$ on the Poincaré section. The distance d_p has been observed to exhibit a strong correlation with the wall shear rate I_p at the instants of the intersection, where $I=\int_0^{L_x}\int_0^{L_z}(\partial u/\partial y|_{y=-h}+\partial u/\partial y|_{y=+h})dxdz/(2L_xL_zU/h)$ is the energy input rate[9] (or equivalently wall shear rate), u being the streamwise velocity. Only if the flow state visits the neighborhood of the periodic orbit, the wall shear rate becomes small. The low wall shear rate is, therefore, a useful indicator of the approach of the state to the periodic orbit. The wall shear rate averaged along the periodic orbit with the period $TU/h=85.3$ ($T^+=248$) is $\overline{I}=1.95$ and much less than that along the turbulent orbit, where $\overline{I}=2.91$ when averaged over $TU/h\approx 2.5\times 10^4$ ($T^+\approx 7.2\times 10^4$). Consistency of $\overline{I}$ has been confirmed between the symmetric and nonsymmetric turbulence.

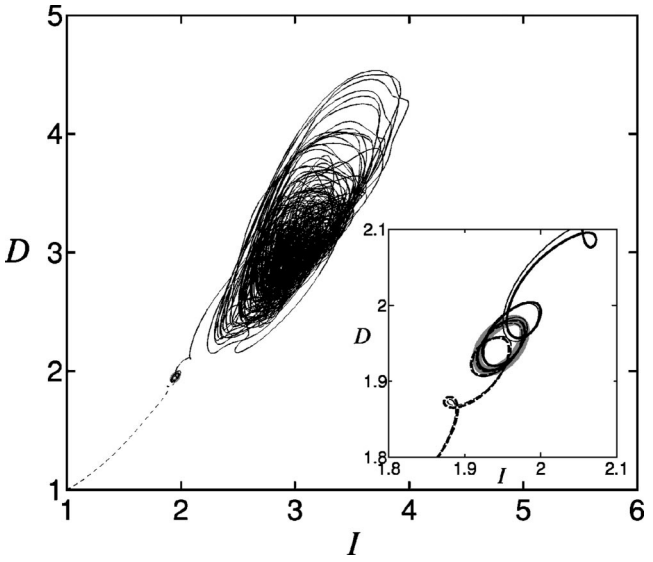

FIG. 1. The (I,D) projection of two trajectories slightly perturbed in the positive (solid line) or negative (dotted line) unstable direction from the periodic orbit. The thick gray closed trajectory is the periodic orbit. The inset is a magnification of the two trajectories around the periodic orbit, in which two other trajectories for the flows under weak spanwise system rotation ($2\Omega h/U=\pm 10^{-4}$) are also shown by thick lines. The thick solid and dotted lines represent the flows under antiparallel (positive) and parallel (negative) rotation to the mean shear vorticity, respectively.

Eigenvalues (i.e., the Floquet multipliers) for the Jacobian matrix, $D_{\boldsymbol{r}}\boldsymbol{f}(\boldsymbol{r}_f)$, on the fixed point (the periodic solution) $\boldsymbol{r}_f$ of the Poincaré map represent the stability characteristics of the periodic solution to infinitesimal disturbances with the same wall-parallel periods and symmetries as those of the periodic solution. It has been found that there is only one (real) unstable eigenvalue $\lambda_u=30.3$ with modulus greater than unity, and all the others are stable. Let $\boldsymbol{e}_u$ denote the unit eigenvector corresponding to the unstable eigenvalue λ_u. The two trajectories shown in Fig. 1 are the two-dimensional projection of the orbits in phase space that start respectively from the initial points $\boldsymbol{r}=\boldsymbol{r}_f\pm\epsilon\|\boldsymbol{r}_f\|\boldsymbol{e}_u$ ($\|\boldsymbol{r}_f\|=0.310$) on the Poincaré section, where $\epsilon=10^{-4}$. The vertical axis denotes the energy dissipation rate[9] $D=\int_0^{L_x}\int_{-h}^{+h}\int_0^{L_z}|\boldsymbol{\omega}|^2dxdydz/(2L_xL_zU^2/h)$, where $\boldsymbol{\omega}$ is the vorticity vector. The (solid) trajectory slightly perturbed in the positive unstable direction $+\boldsymbol{e}_u$ from the (thick gray) periodic orbit tends to the turbulent state, while the (dotted) one perturbed in the negative unstable direction $-\boldsymbol{e}_u$ tends to the laminar state $(I,D)=(1,1)$. This means that the periodic orbit and its local stable manifold form the separatrix between the basin of attraction of the turbulent and the laminar states. The information on such a

basin of attraction is of great importance not only for elucidation of transition mechanisms but also for controlling turbulent flows. In general, however, it is difficult to extract a basin boundary because it should be very complicated in high-dimensional phase space. Here the discovery of the periodic orbit leads us to find the local basin boundary. In the following we shall discuss a laminarization method for the minimal Couette turbulence based upon the knowledge of the separatrix of the basin of attraction.

Let us introduce the new scalar parameter σ for controlling the flow, which can be varied in a small range about $\sigma=0$. The periodic orbit corresponds to the fixed point of the new map $\boldsymbol{f}(\boldsymbol{r},\sigma)$ for $\sigma=0$, i.e., $\boldsymbol{r}_f=\boldsymbol{f}(\boldsymbol{r}_f,0)$. Supposing that the turbulent state is visiting the vicinity of the periodic orbit, we linearize the map about the fixed point $(\boldsymbol{r}_f,0)$ as

$$\boldsymbol{r}^{i+1}-\boldsymbol{r}_f=D_{\boldsymbol{r}}\boldsymbol{f}(\boldsymbol{r}_f,0)(\boldsymbol{r}^i-\boldsymbol{r}_f)+D_\sigma\boldsymbol{f}(\boldsymbol{r}_f,0)\sigma^i, \tag{1}$$

where the superscript i $(=0,1,\ldots)$ indicates variables at the ith return. A product between the vector $\boldsymbol{v}_u$ (pointing towards the interior of the turbulent basin), for which $\boldsymbol{v}_u\cdot\boldsymbol{v}_s=0$ for all vectors $\boldsymbol{v}_s$ lie in the local stable manifold, and Eq. (1) yields

$$\boldsymbol{v}_u\cdot(\boldsymbol{r}^{i+1}-\boldsymbol{r}_f)=\lambda_u[\boldsymbol{v}_u\cdot(\boldsymbol{r}^i-\boldsymbol{r}_f)]+\sigma^i[\boldsymbol{v}_u\cdot D_\sigma\boldsymbol{f}(\boldsymbol{r}_f,0)].$$

In the present method for laminarization, accordingly, when the turbulent state approaches the periodic orbit, we impose $\sigma^0\neq0$ only until the first return $i=1$ by

$$\sigma^0=-c\lambda_u[\boldsymbol{v}_u\cdot(\boldsymbol{r}^0-\boldsymbol{r}_f)]/[\boldsymbol{v}_u\cdot D_\sigma\boldsymbol{f}(\boldsymbol{r}_f,0)], \tag{2}$$

where $c>1$ so that the state point can go beyond the stable manifold toward the laminar state. This strategy can be extended to the case of more than one unstable direction. In the Ott–Grebogi–Yorke (OGY) method[4] for stabilization, on the other hand, σ^i is determined at each return $i=0,1,\ldots$ by the same Eq. (2) but for $c=1$ so that the state point can fall on the stable manifold. In Eq. (2) we have assumed that $\boldsymbol{v}_u\cdot D_\sigma\boldsymbol{f}(\boldsymbol{r}_f,0)\neq0$. It is confirmed that spanwise system rotation satisfies this condition (see the inset in Fig. 1), and thus we introduce the uniform system rotation vorticity 2Ω as an example of possible parameters.

Figure 2 shows the results of laminarization tests. The system rotation 2Ω determined by Eq. (2) for $c=2$ is imposed for a short interval between the zeroth and first returns if the turbulent state approaches the periodic orbit (i.e., $d_p<0.15$ at $i=0$). We can see that the laminarization is achieved for the low wall shear rate $I_p\lesssim2.2$ which was observed above to be a measurable indicator. The weaker rotation is sufficient for the laminarization of the flow with the lower wall shear rate. The linear theory does not seem to be applied to the state with $I_p\gtrsim2.2$ (which roughly corresponds to $d_p\gtrsim0.1$). The condition of the achievement of stabilization by the OGY method[4] has been found to be much stricter, i.e., $d_p\lesssim10^{-2}$.

In the above laminarization method we need to know the state vector $\boldsymbol{r}^0$ which could not be measured in real applications. However, a trivial upper bound of $2|\Omega|$ for fixed $\|\boldsymbol{r}^0-\boldsymbol{r}\|$ is given at the case that $\boldsymbol{v}_u$ is parallel to $\boldsymbol{r}^0-\boldsymbol{r}$, and there should exist some small constant value of 2Ω sufficient for the laminarization of all the possible states with small I_p. Taking into account the results in Fig. 2, if $I_p<2.1$ we impose the system rotation of the *constant* $2\Omega h/U(=-3\times10^{-3})$ on the minimal Couette turbulence without imposing the symmetries (i) and (ii). The rotation is imposed for a *constant* time, which is set to be the same as the period $(T^+=248)$ of the periodic solution. This method has been tested against three different turbulent states, and in all the cases the turbulent flow has laminarized [see Fig. 3 (thick dashed line) for one of the three]. The imposed rotation is so weak that the total rotation angle ΩT is only 7.3°. In Fig. 3 the rotation is turned on at $t^+_{\rm on}=0$, but the laminarization is also accomplished for $-100\lesssim t^+_{\rm on}\lesssim20$. For $t^+_{\rm on}=0$, it has been found that the time interval of the rotation can be reduced to

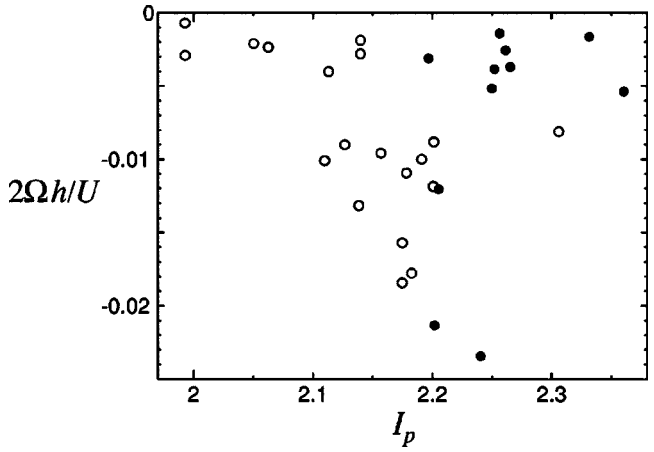

FIG. 2. The values of the system rotation vorticity 2Ω used for laminarization tests [Eq. (2) with $c=2$] vs the wall shear rate I_p at the instants of the zeroth return. The open (closed) circles denote success (failure) in laminarization.

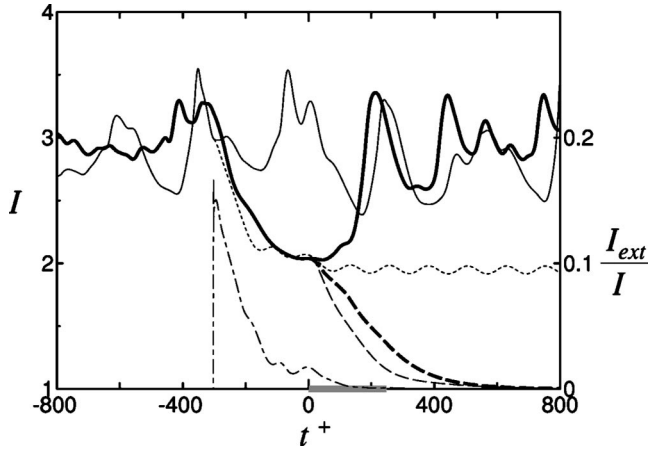

FIG. 3. Time evolution of the wall shear rate I for uncontrolled and controlled flows. The thick and thin solid lines represent the two uncontrolled flows. One of them, shown by the thick solid line, approaches the periodic orbit naturally, and during its natural approach $(t^+=0)$ the system rotation is turned on. The thick dashed line represents the corresponding controlled flow. The other (the thin solid line) does not approach the periodic orbit, but if Pyragas' external force with $kh/U=0.1$ is turned on at $t^+=-302$, the corresponding state, denoted by the thin dotted line, approaches the periodic orbit. During this forced approach $(t^+=0)$ the system rotation is turned on, and the corresponding controlled flow is shown by the thin dashed line. The dotted-dashed line denotes the energy input $I_{\rm ext}$ through Pyragas' forcing normalized with I. The system rotation is imposed for the period shown by the thick gray segment.

$T^+ \approx 100$. Note that in this method only the wall shear rate needs to be known for the laminarization.

Although the turbulent state occasionally visits the neighborhood of the periodic orbit, a close approach is not frequent (the mean time interval between successive close approaches of $I_p < 2.2$ is $T^+ \approx 4 \times 10^4$). The close approach might be rarer at a higher Reynolds number or in a larger computational domain.[12] Hence a laminarization method without waiting until the close approach is desired, and next we briefly discuss such a method. In order to let the turbulent state approach the periodic orbit at any time, we implement the external force $k\mathcal{P}(\boldsymbol{u}_p - \boldsymbol{u})$ per unit mass in the Navier–Stokes equation by following Pyragas' method,[5] where k is a (positive) scalar gain, and $\boldsymbol{u}_p$ and $\boldsymbol{u}$ are the velocities of the periodic flow and the flow to be controlled, respectively. The projection operator $\mathcal{P}$ provides the reconstitution of a solenoidal velocity field given by the Fourier–Chebyshev coefficients of the wall-normal velocity and vorticity, $\tilde{v}_{m,l,m'}$ and $\tilde{\omega}_{ym,l,m'}$, *only* for $(m,m') = (0,\pm 1)$, $(\pm 1,0)$, $(\pm 1,\pm 1)$, $(\pm 1 \mp 1)$, and $l = 0,2$. Note that the number of degrees of freedom of the external force is much lower than that of the system, N. Here we use the external force localized in the Fourier–Chebyshev space, although spatially localized pinning control[6] was also applied to two-dimensional turbulence. The external force can globally stabilize the periodic orbit. Actually, if we turn on the forcing at any instant, the turbulent state immediately tends to the periodic orbit as shown in Fig. 3 (thin dotted line). After the close approach ($I_p < 2.1$), the laminarization has been achieved in the same way as above (thin dashed line). The time needed for the approach depends on turbulent states and its mean value is $\overline{T^+} \approx 300$.

In this Letter a laminarization strategy has been presented for a plane Couette system, where the unstable periodic solution plays a crucial role. To extend this strategy to minimal turbulent channel flows, we need the same kind of nonlinear solution to a plane Poiseuille system. Such solutions have already been found in the Poiseuille system at subcritical Reynolds numbers by Itano and Toh[10] and Waleffe[8] who have reported that their traveling-wave solutions are on the separatrix between the basin of attraction of turbulent and laminar states. Their solutions could be a good candidate for the base of laminarization. In the supercritical Poiseuille system, however, the laminarization demands stabilization of a laminar state. The stability characteristics of the periodic solution to spatially subharmonic disturbances should be investigated for implementation of the present laminarization strategy in full plane Couette turbulence, and the investigation is left for a future study.

The author would like to express his thanks to Professor M. Nagata and Professor S. Kida for their encouragement, and Professor S. Toh for providing him a simulation code. This work was supported in part by a Grant-in-Aid for Scientific Research from the Japan Society for the Promotion of Science and by the Center of Excellence for Research and Education on Complex Functional Mechanical Systems (COE program of the Ministry of Education, Culture, Sport, Science and Technology of Japan).

[1] J. Kim, "Control of turbulent boundary layers," Phys. Fluids **15**, 1093 (2003).
[2] T. R. Bewley, P. Moin, and R. Temam, "DNS-based predictive control of turbulence: an optimal benchmark for feedback algorithms," J. Fluid Mech. **447**, 179 (2001).
[3] M. Högberg, T. R. Bewley, and D. S. Henningson, "Relaminarization of $Re_\tau = 100$ turbulence using gain scheduling and linear state-feedback control," Phys. Fluids **15**, 3572 (2003).
[4] E. Ott, C. Grebogi, and J. A. Yorke, "Controlling chaos," Phys. Rev. Lett. **64**, 1196 (1990).
[5] K. Pyragas, "Continuous control of chaos by self-controlling feedback," Phys. Lett. A **170**, 421 (1992).
[6] S. Guan, Y. C. Zhou, G. W. Wei, and C.-H. Lai, "Controlling flow turbulence," Chaos **13**, 64 (2003).
[7] M. Nagata, "Three-dimensional finite-amplitude solutions in plane Couette flow: bifurcation from infinity," J. Fluid Mech. **217**, 519 (1990).
[8] F. Waleffe, "Homotopy of exact coherent structures in plane shear flows," Phys. Fluids **15**, 1517 (2003).
[9] G. Kawahara and S. Kida, "Periodic motion embedded in plane Couette turbulence: regeneration cycle and burst," J. Fluid Mech. **449**, 291 (2001).
[10] T. Itano and S. Toh, "The dynamics of bursting process in wall turbulence," J. Phys. Soc. Jpn. **70**, 703 (2001).
[11] J. Jiménez and M. P. Simens, "Low-dimensional dynamics in a turbulent wall flow," J. Fluid Mech. **435**, 81 (2001).
[12] J. Jiménez, G. Kawahara, M. P. Simens, M. Nagata, and M. Shiba, "Characterization of near-wall turbulence in terms of equilibrium and bursting solutions," Phys. Fluids **17**, 015105 (2005).
[13] J. M. Hamilton, J. Kim, and F. Waleffe, "Regeneration mechanisms of near-wall turbulence structures," J. Fluid Mech. **287**, 317 (1995).